



Experimental study of asymmetric multi-pass spinning

Yong Xiao^{1,2} · Zhiren Han^{1,2} · Shuyang Zhou^{1,2} · Zhen Jia²

Received: 11 August 2019 / Accepted: 9 August 2020 / Published online: 15 August 2020
© Springer-Verlag London Ltd., part of Springer Nature 2020

Abstract

Various approaches to produce non-axisymmetric parts in metal spinning have been developed by researchers. In asymmetric multi-pass spinning, the motion of the roller is synchronized with the mandrel's rotation by CNC codes to achieve oblique or non-circular shapes. In this study, cylindrical cups are formed using two kinds of oblique pass sets to investigate the effects of different parameters on thickness distribution and forming limit. In the translational pass set, the inclination angle is determined by the difference of the wall depths on two sides of the product and it is determined by the difference of half cone angles in the rotational pass set. The difference of wall thickness distribution in the translational pass is greater than that in the rotational pass and it increases as the inclination angle increases. The difference between the axial distributions on two sides of the wall decreases as the pass pitch increases near the top of the product, and it increases near the edge of the wall. A greater incremental angle does not affect the difference but reduces the uniformity of the wall thickness in the rotational pass set. All the failures are wrinkles in the experiments. Wrinkles occur when the pass pitch or the roller feed ratio is too large. A greater inclination angle reduces the forming limit in the translational pass set and does not affect the forming limit in the rotational pass set.

Keywords Metal spinning · Asymmetric spinning · Multi-pass spinning · Thickness distribution · Tool path

1 Introduction

Metal spinning is one of the metal forming processes which transform flat sheet metal blanks into axisymmetric hollow shapes. It is widely used for producing round metal parts for the aerospace and automotive industries, musical instruments, and kitchenware. It has a number of advantages when compared with other forming techniques such as deep drawing or press forming. The products usually have high-quality surface and mechanical strength. It requires low forming forces for the high-strength material and has a low tooling cost. Simple and non-dedicated tooling provides flexibility and shapes with complex geometries.

In recent years, advanced methods, which enable the non-circular shapes, are developed to overcome the

limitation of traditional spinning. Amano and Tamura [1] successfully formed an elliptical shape by synchronizing the roller's motion with the rotation of the spindle by using a mechanical cam. This method shows weak accuracy due to the difficulty of achieving the desired roller-mandrel clearance. Gao et al. [2] used an offset mandrel to produce elliptical parts. The study showed that the thickness varies by 10% in conventional spinning and it agrees with the sine-law in mandrel-free shear spinning. Xia et al. [3] developed a method called “profile driving,” in which the motion of the roller and the rotation of the mandrel are synchronized using cams and gears, to produce noncircular-hollow-cone shapes.

The methods above require a set of dedicated equipment for one type of product. Researchers have developed flexible methods for non-circular shapes using more advanced techniques. Arai [4] conducted experiments for non-circular shapes and offset cross sections in force-controlled spinning. This method does not need a dedicated mechanism for each shape. Different shapes of the product can be easily spun by replacing the mandrel. Jia et al. [5] investigated the mechanism of square section die-less spinning. Numerical simulations and experiments were conducted to investigate the distributions of stress, strain, and wall thickness. This method

✉ Zhiren Han
hanren888@163.com

¹ School of Mechanical Engineering, Northwestern Polytechnical University, Xi'an 710072, Shaanxi, China

² Key Lab of Fundamental Science for National Defense of Aeronautical Digital Manufacturing Process, Shenyang Aerospace University, Shenyang 110136, China

Fig. 1 PS-CNCXY600-5 NC spinning lathe: **a** full view of the lathe and **b** working portion of spinning



enables the formation of square section cones. However, the result could not meet the design shape since the edges of the cross section appeared to be arcs. Sugita and Arai [6] developed synchronous multi-pass spinning which enables non-circular sections with straight walls. The material built-up at the corner of the side wall causing thickness increases. Forming limits using two kinds of pass sets were investigated.

Another type of asymmetric spinning enables the formation of oblique shapes. Sekiguchi and Arai [7] proposed an oblique spinning method to control the thickness distribution in shear spinning. The motion of the roller was controlled in both axial and radial directions. Synchronous die-less spinning and force-controlled spinning methods were used in the experiments. The results showed that the wall thickness distribution nearly coincided with the sine law. Han et al. [8] adopted this method and conducted a series of experiments to investigate the thickness distributions of oblique cones

in die-less shear spinning. The roller path was analyzed and deduced in detail. The result showed that the thickness distributions of the products are basically in agreement with the theoretical value. Arai and Kanazawa [9] proposed a method for non-circular shapes with oblique bottoms. The forming limits using different path designs and the effect of the process parameters on the result were investigated. The circumferential distributions of thickness could not be equalized without an intermediate shape. Xiao et al. [10] developed an asymmetric multi-pass spinning method that enables the formation of oblique cylinder shape with a planar flange. Experiments on thickness distribution and forming limits are carried out. However, the thickness distributions of the products could not be well-controlled and appeared to be non-uniform.

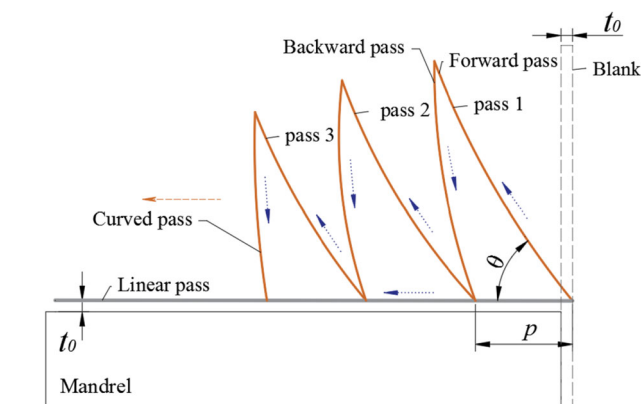


Fig. 2 Translational pass set

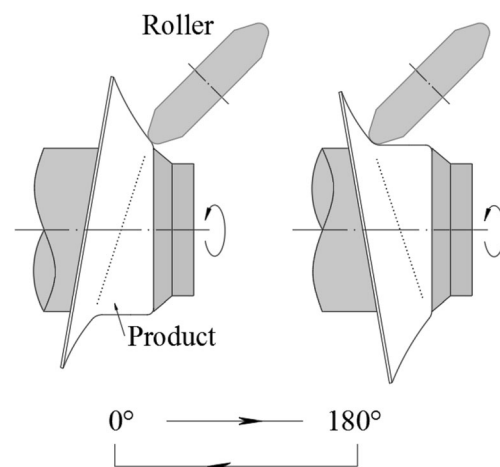


Fig. 3 The motion of the roller during one revolution of the spindle

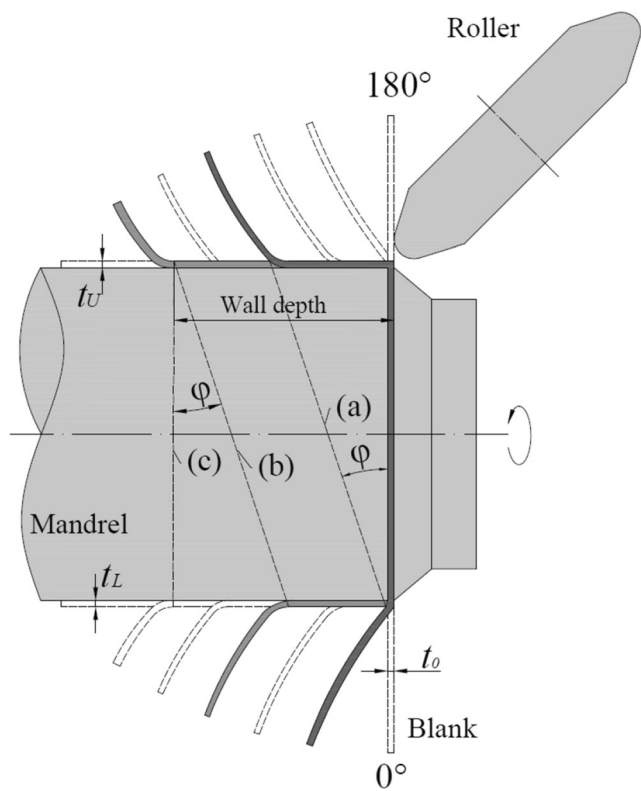


Fig. 4 Forming process of asymmetric spinning using the translational pass set

In conventional spinning, the circumferential distribution of thickness on the products is uniform since the cross-section being formed is axisymmetric. In contrast, the thickness varies circumferentially for non-circular spinning or oblique spinning. In this study, forming experiments on cylindrical shapes using two kinds of pass sets in multi-pass asymmetric spinning are conducted to investigate the effect of different parameters on the forming result.

2 Experimental setup

Figure 1 shows photographs of a computer numerical controlled spinning lathe (PS-CNCSXY600-5) used in this study.

Table 1 Parameters of the cylindrical cup using the translational pass set in asymmetric spinning

Parameters	Values
Pass angle θ ($^{\circ}$)	60
Pass pitch p (mm)	2, 4, 6, 8
Inclination angle φ ($^{\circ}$)	13, 24, 37
Roller feed ratio f (mm/rev)	1

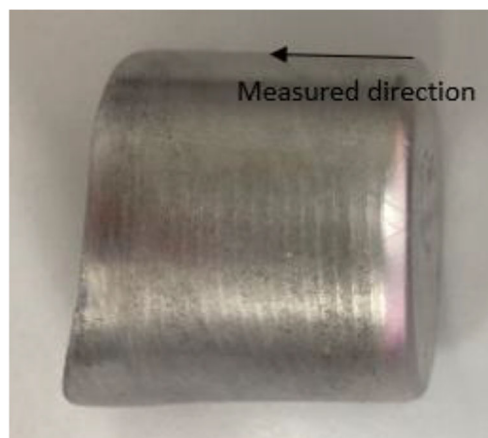


Fig. 5 Example of formed products using the translational pass set

The spindle is driven by an 11 kW servomotor, and the axial and radial motion of the roller is controlled by two sophisticated servomotors with a positional accuracy of 0.02 mm. The blank is clamped in the center by a mandrel and a tailstock. The tailstock rotates along with the mandrel which is driven by the spindle. Since the motion of the roller is synchronized with the rotation of the spindle, the spindle speed is much slower than that in conventional spinning which is 30 rpm in this study. The diameter of the roller is 110 mm and the nose radius is 6 mm. The roller is inclined by 45° to the spindle axis.

Circular disks made of aluminum alloy (6061) with a diameter of 100 mm and a thickness 1.2 mm was used as blank sheets in this study. The diameter of the cylindrical mandrel is 50 mm. The spinning ratio in the experiments is 2. The thicknesses of the products were measured using a micrometer with an accuracy of 0.01 mm.

3 Translational pass

3.1 Toolpath design

In the translational pass set, each curved pass is composed of a forward pass and a backward pass as shown in Fig. 2. Pass angle θ is the angle of the endpoint relative to the start point of a forward pass. The forward pass is shifted by a pass pitch (p mm) keeping θ constant. A forward pass is used to change the shape of the flange and the material is pushed back onto the mandrel by a backward pass. The linear pass is used at the end of the process to push the wall on the mandrel.

In asymmetric spinning, the blank rotates around the spindle axis; the position of the roller is controlled synchronously in both radial and axial directions during one revolution of the mandrel. When the mandrel rotates from 0° to 180° , the roller moves from the top to the open end of the product in axial

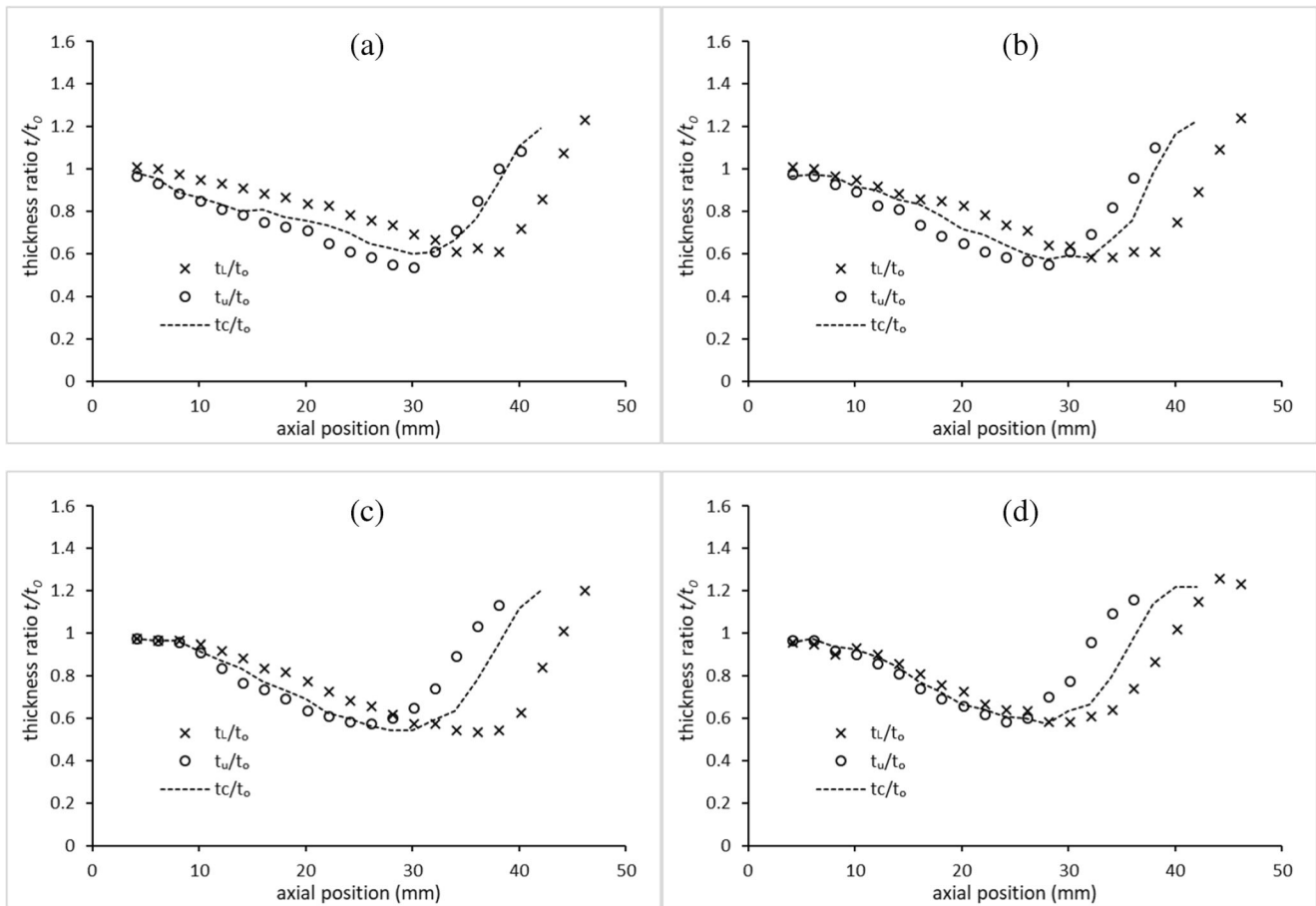


Fig. 6 Axial distributions of thickness ratio along two sides of the wall when $\varphi = 24^\circ$: **a** $p = 2$ mm, **b** $p = 4$ mm, **c** $p = 6$ mm, and **d** $p = 8$ mm

direction, and the roller moves back axially when the mandrel rotates from 180° to 0° as shown in Fig. 3. Figure 4 shows the forming process using the translational pass set in asymmetric spinning. First, the product is formed from a sheet blank to

shape (a) with an inclination angle φ by achieving different depths of the wall on two sides of the product. Next, the shape of the product is changed to (b) by keeping φ constant. Finally, φ is reducing to zero by achieving shape (c). The

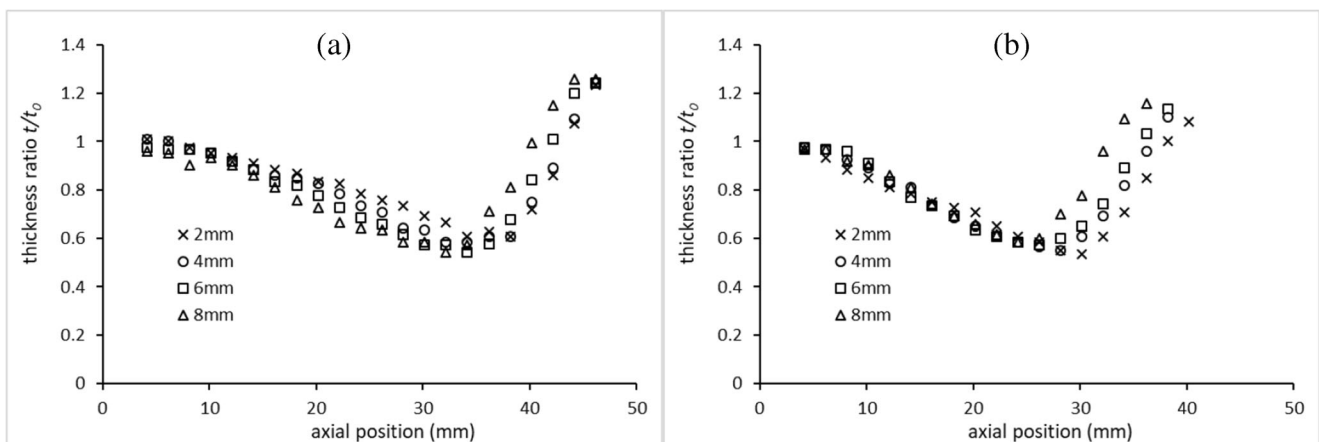


Fig. 7 Axial distributions of thickness ratio along two sides of the wall with different p when $\varphi = 24^\circ$: **a** lower side and **b** upper side

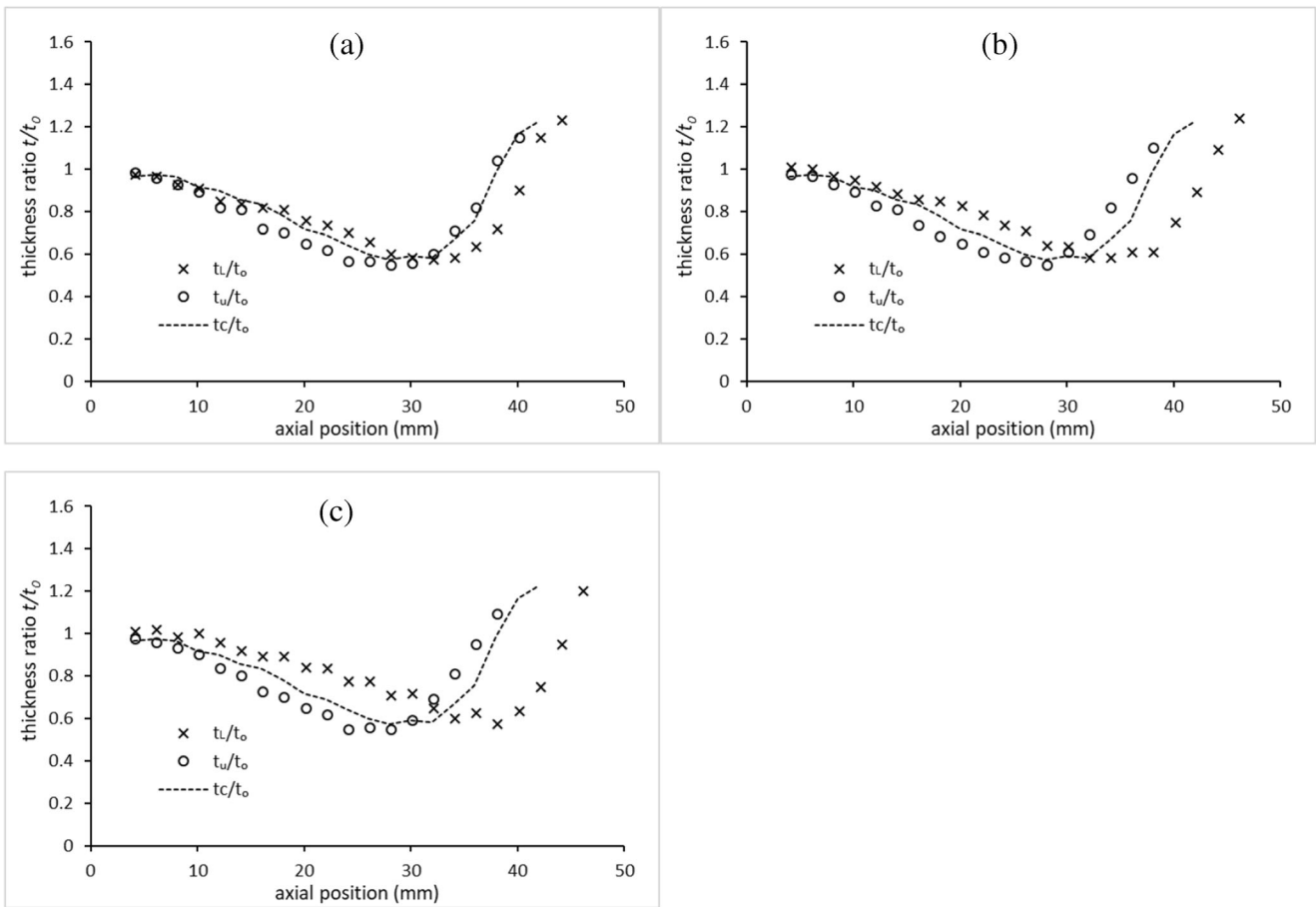


Fig. 8 Axial distributions of thickness ratio along two sides of the wall when $p = 4$ mm: **a** $\varphi = 13^\circ$, **b** $\varphi = 24^\circ$, and **c** $\varphi = 37^\circ$

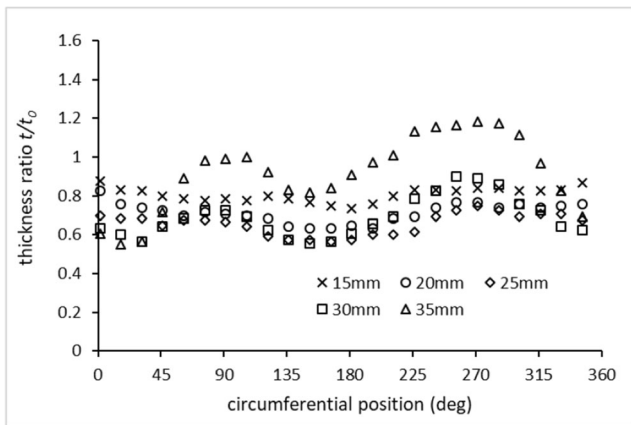


Fig. 9 Circumferential distributions of thickness ratio at different positions on the wall

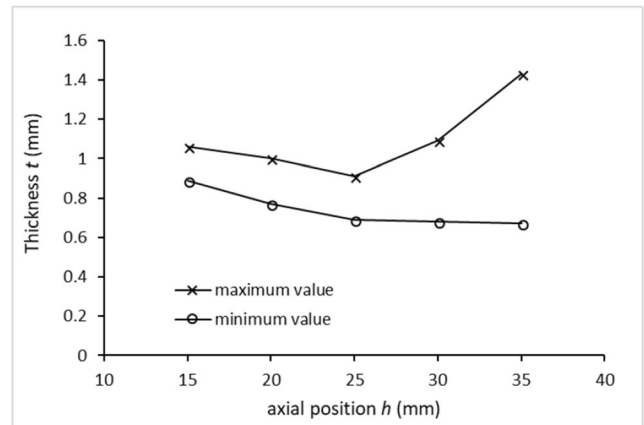


Fig. 10 Maximum and minimum values of circumferential thickness at different positions on the wall

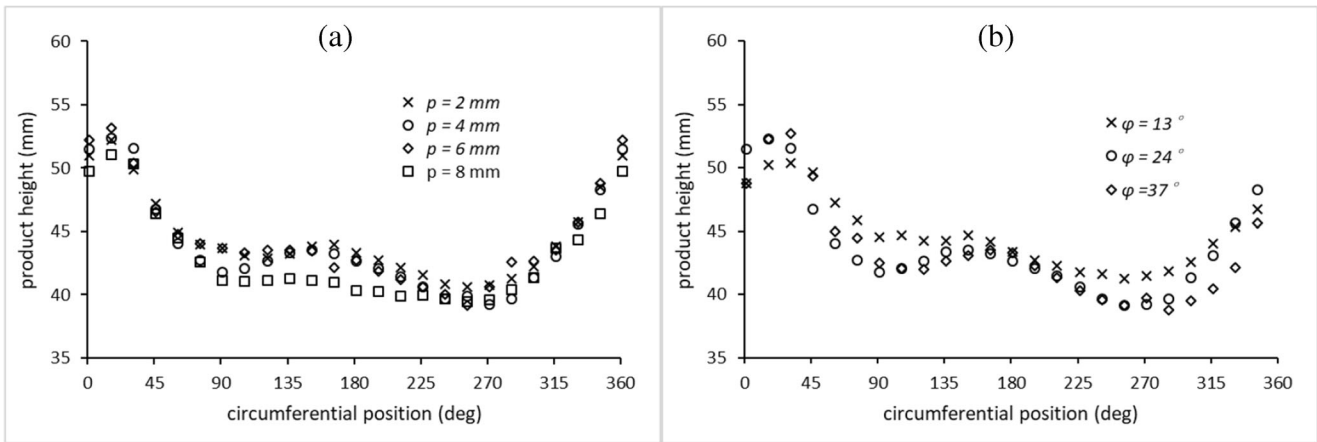


Fig. 11 Circumferential distributions of product heights: **a** with different p when $\varphi = 24^\circ$ and **b** with different φ when $p = 4$ mm

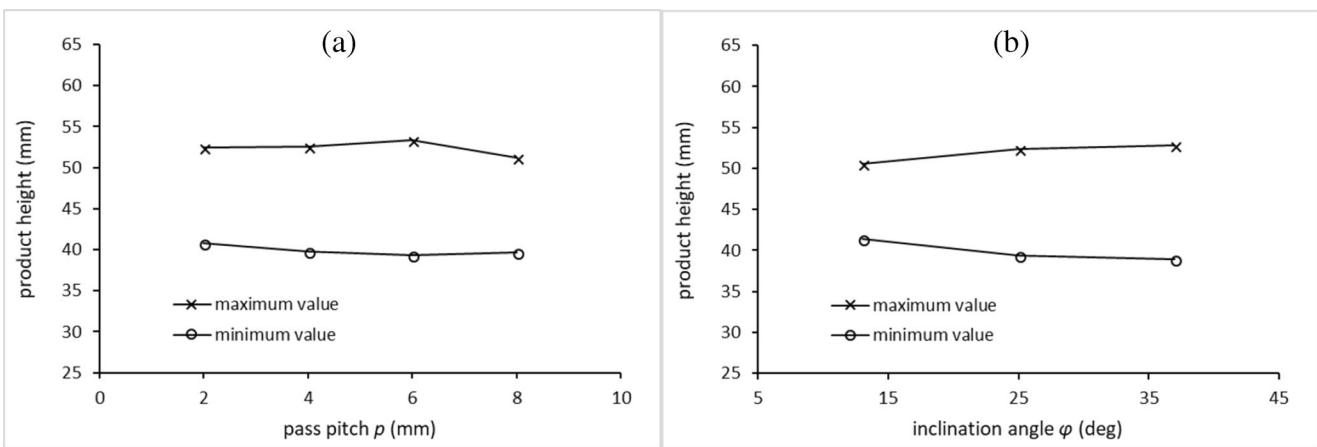


Fig. 12 Maximum and minimum values of circumferential product heights: **a** with different p when $\varphi = 24^\circ$ and **b** with different φ when $p = 4$ mm

product is formed without a flange; all the material is pushed on the mandrel in the end.

3.2 Axial distribution of wall thickness

The experiments on cylindrical cups using the translational pass set in asymmetric spinning were conducted with the pa-

Fig. 13 Examples of failed products using the translational pass set



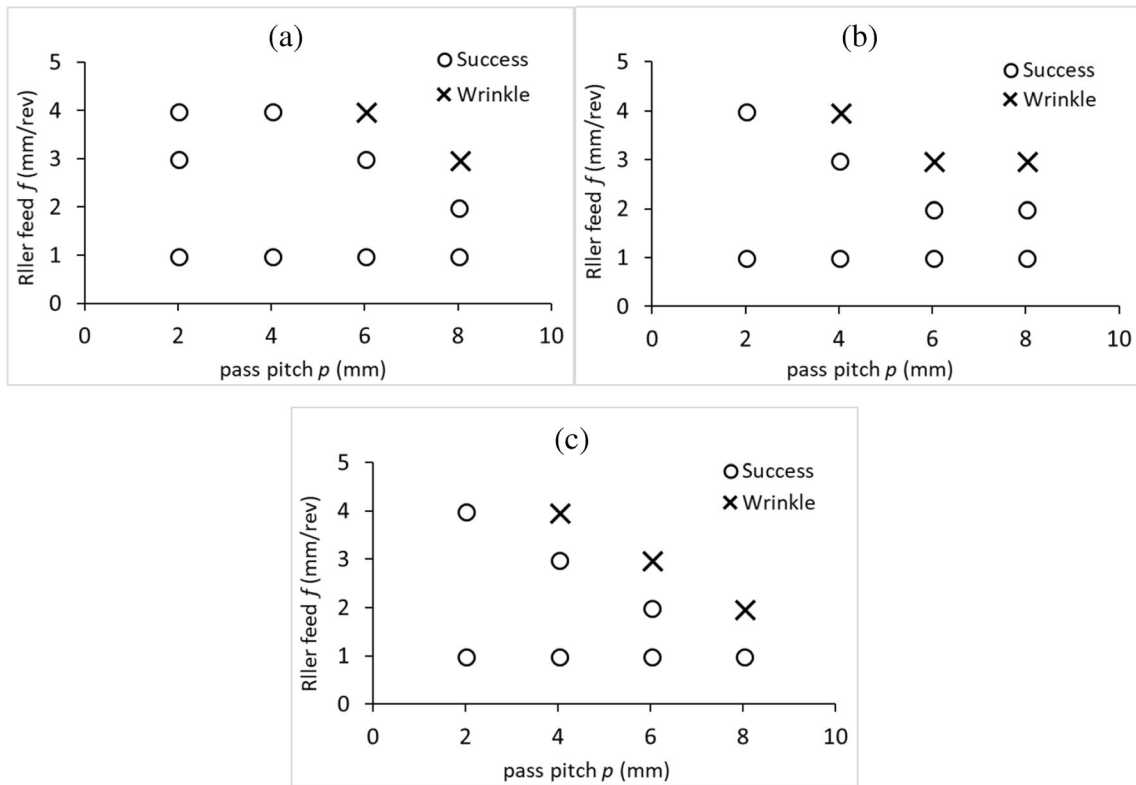


Fig. 14 Forming limit with different combinations of parameters: $\varphi = 13^\circ$, $\varphi = 24^\circ$, and $\varphi = 37^\circ$

rameters given in Table 1. For comparison, cylindrical cups using the same pass set in conventional spinning were formed.

Figure 5 shows an example of the formed products using the translational pass set in asymmetric spinning. The thickness on the upper and lower sides of the wall (t_U and t_L as

shown in Fig. 4) was measured axially. Figure 6 shows the axial distribution of wall thickness ratios (t_U/t_0 and t_L/t_0) with different pass pitches $p = 2, 4, 6,$ and 8 mm. The dotted lines are distributions of thickness ratio (t_C/t_0) in conventional spinning (when $\varphi = 0^\circ$). The shape of t_U/t_0 is shifted leftwards and t_L/t_0 is shifted rightwards when compared with t_C/t_0 . Due to

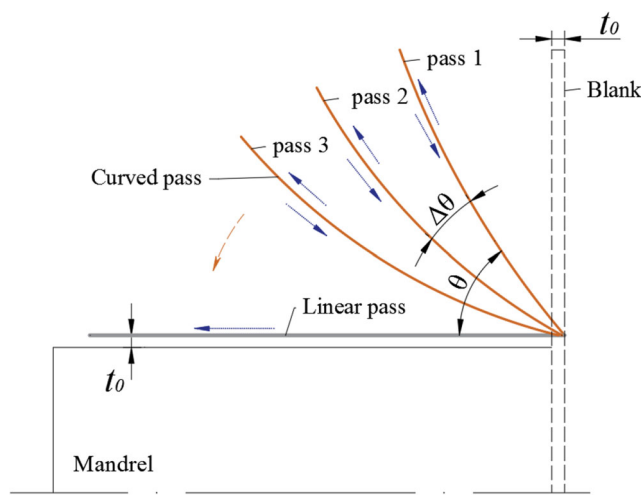


Fig. 15 Rotational pass set

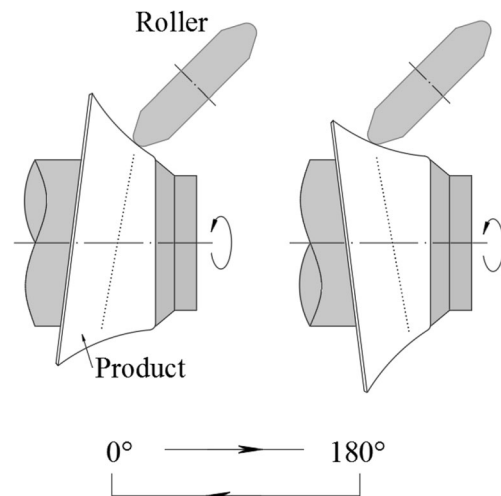


Fig. 16 The motion of the roller during one revolution of the spindle

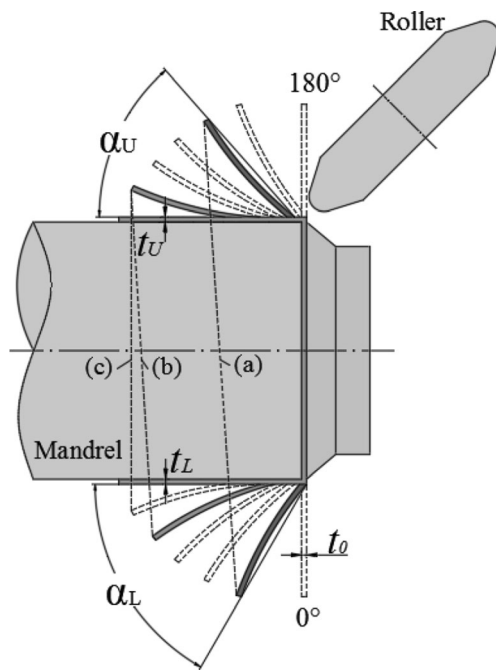


Fig. 17 Forming process of asymmetric spinning using the rotational pass set

the inclination angle, material tends to flow towards the lower side of the wall at the beginning of the process which causes the different thickness distributions. The difference between t_U/t_0 and t_L/t_0 decreases as p increases near the top of the product, and it increases near the edge of the wall except when $p = 8$ mm as shown in Fig. 6a–d. Slight wrinkles were observed during the process when $p = 8$ mm which may interfere with the material flow. The thickness distributions on each side of the product with different p are compared in Fig. 7. The wall thickness is thinner at the beginning and thicker at the end of the product when a larger p is used. Figure 8 shows the axial distribution of wall thickness ratios (t_U/t_0 and t_L/t_0) with different inclination angles $\varphi = 13^\circ, 24^\circ, 37^\circ$. The difference between t_U/t_0 and t_L/t_0 increases as the inclination angle

Table 2 Parameters of the cylindrical cup using the rotational pass set in asymmetric spinning

Parameters	Values
Initial pass angle θ ($^\circ$)	80
Incremental angle $\Delta\theta$ ($^\circ$)	3, 4, 5, 6
Inclination angle φ ($^\circ$)	6, 24, 48, 72
Roller feed ratio f (mm/rev)	1

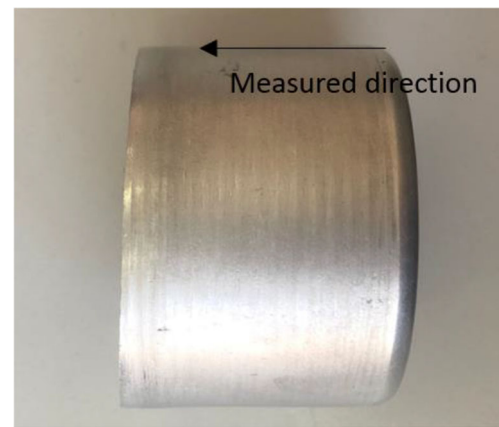


Fig. 18 Example of formed products using the rotational pass set

increases. This indicates that a larger φ reduces the uniformity of the thickness distribution.

3.3 Circumferential distribution of wall thickness

Figure 9 shows circumferential distributions of wall thickness ratio (t/t_0) with parameters of $\varphi = 24^\circ$ and $p = 4$ mm at distances of $h = 15, 20, 25, 30,$ and 35 mm from the top of the product. The circumferential distributions of t/t_0 are not symmetric as the roller's trajectory due to the roller's back-and-forth movement in axial direction. This phenomenon is similar to the forming process of angled-flange cylinder [10]. The maximum and the minimum values of circumferential thickness ratio do not always show up at 0° or 180° direction on the wall as they do in oblique shear spinning [7]. At $h = 30$ mm and $h = 35$ mm, the local maximum values of thickness ratio show up around 90° and 270° and the local minimum values show up around 30° and 150° on the wall, whereas at $h = 15$ mm, 20 mm, and 25 mm, it does not have the same pattern. The maximum and minimum values of circumferential thickness are illustrated in Fig. 10. The range of circumferential distribution of t/t_0 is similar (around 0.2 mm) when $h = 15, 20, 25$ mm and it increases when $h = 30$ and 35 mm due to the increase of the maximum value. The result shows that the circumferential distribution of wall thickness cannot be well-controlled by this method.

3.4 Product height

Figure 11 shows the circumferential distributions of heights of the products formed with parameters of $\varphi = 13^\circ, 24^\circ, 37^\circ$ and $p = 2, 4, 6, 8$ mm. The maximum and minimum values are shown in Fig. 12. The distributions of product heights have

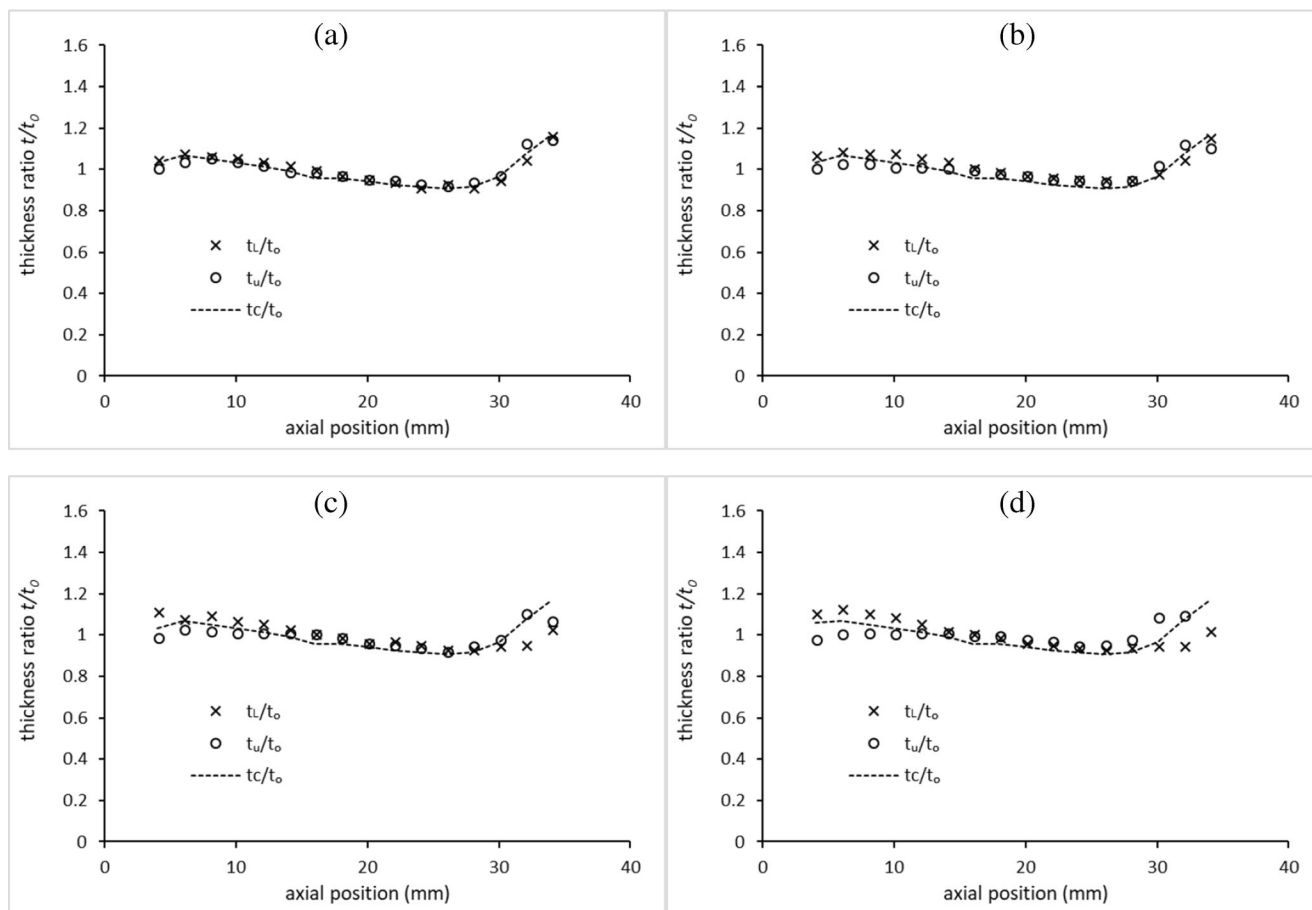


Fig. 19 Axial distributions of thickness ratio along two sides of the wall with different φ when $\Delta\theta = 3^\circ$: **a** $\varphi = 6^\circ$, **b** $\varphi = 24^\circ$, **c** $\varphi = 48^\circ$, and **d** $\varphi = 72^\circ$

wavy shapes. The local minimum values of product heights show up around 90° and 270° directions and the local maximum values show up around 30° and 150° directions. The distributions are similar when $p = 2, 4,$ and 6 mm; there is an obvious decrease of the height when $p = 8$ mm as shown in Fig. 11a. A greater φ could get smaller product heights as shown in Fig. 11b. The range of product heights increases slightly as p increases when $p = 2, 4,$ and 6 mm as shown in Fig. 12a. The range of product heights increases as φ increases as shown in Fig. 12b.

3.5 Forming limit

Figure 13 shows the examples of failed products using the translational pass set. All the failures are wrinkles in these experiments and no fracture was observed. Forming limit experiments were conducted with parameters of $f = 1, 2, 3, 4$ mm/rev, $\varphi = 13^\circ, 24^\circ, 37^\circ$, and $p = 2, 4, 6, 8$ mm. The success and failure of the forming results are illustrated in Fig. 14.

Wrinkles are more likely to occur as $p, f,$ and φ increases. Wrinkles occurred at the end of the process when p was 4 mm and 6 mm due to the elongation of the wall around 0° directions. When p was 8 mm, wrinkles occurred at the beginning of the process due to the large pass pitch.

4 Rotational pass

4.1 Toolpath design

In the rotational pass set, the roller is moving forward and backward in each curved pass as shown in Fig. 15. Pass angle θ is the angle of the endpoint relative to the start point of a pass. It decreases by an incremental angle $\Delta\theta$ for each pass relative to the last pass. The linear pass is used at the end of the process to push the wall on the mandrel.

The position of the roller is controlled synchronously in both radial and axial directions during every revolution of

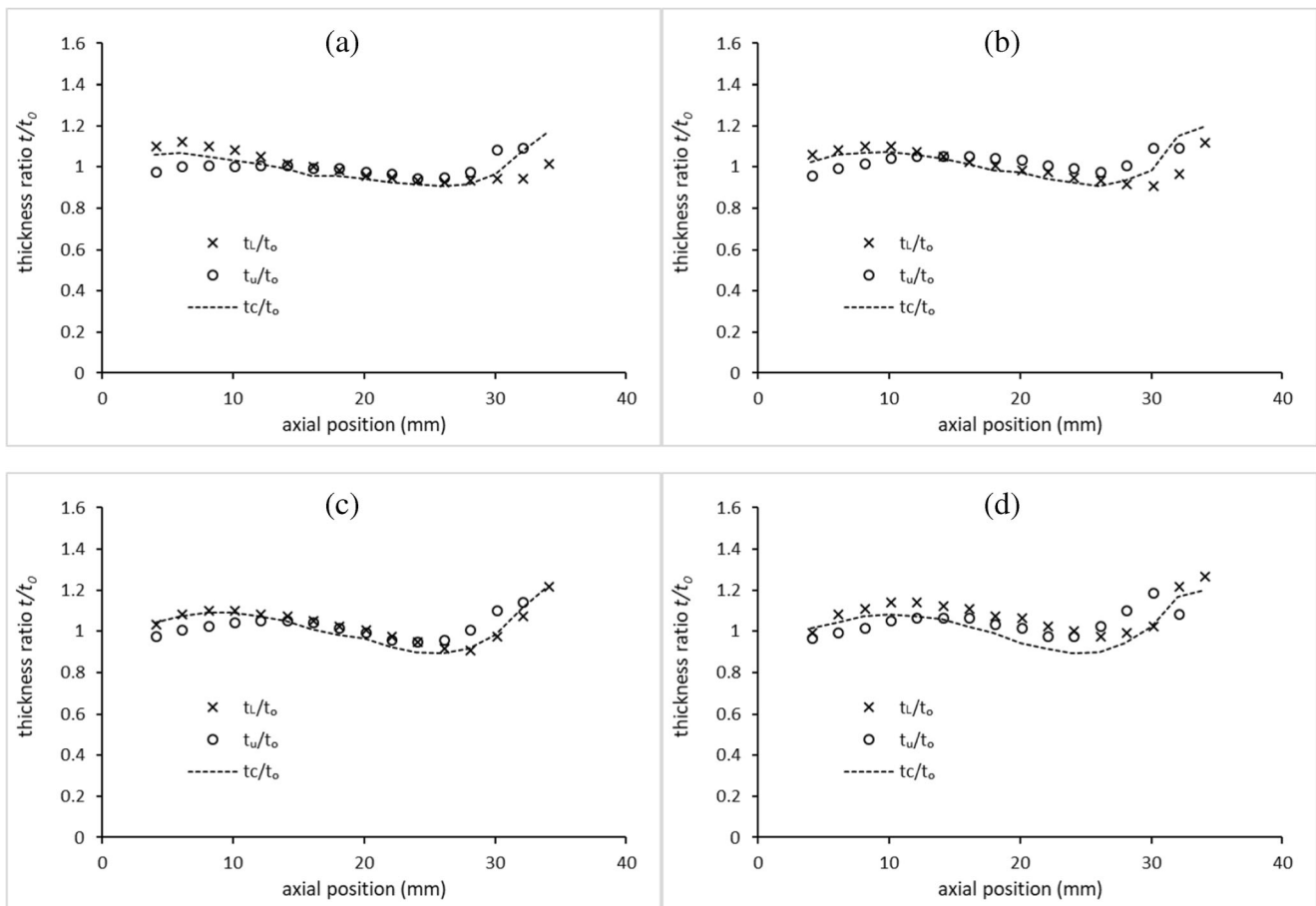


Fig. 20 Axial distributions of thickness ratio along two sides of the wall with different $\Delta\theta$ when $\varphi = 72^\circ$: **a** $\Delta\theta = 3^\circ$, **b** $\Delta\theta = 4^\circ$, **c** $\Delta\theta = 5^\circ$, and **d** $\Delta\theta = 6^\circ$

the spindle to achieve the asymmetric shape as illustrated in Fig. 16. The forming process using the rotational pass set in asymmetric spinning is shown in Fig. 17. The inclination angle φ is determined by the difference of half cone angle on each side of the product ($\varphi = \alpha_L - \alpha_U$). The product is formed

from a sheet blank to shape (a) with an inclination angle φ . Then, the shape of the product is changed to (b) by keeping φ constant. Next, φ is reduced to zero by achieving shape (c). Finally, a linear pass is used to force the wall of the product onto the mandrel.

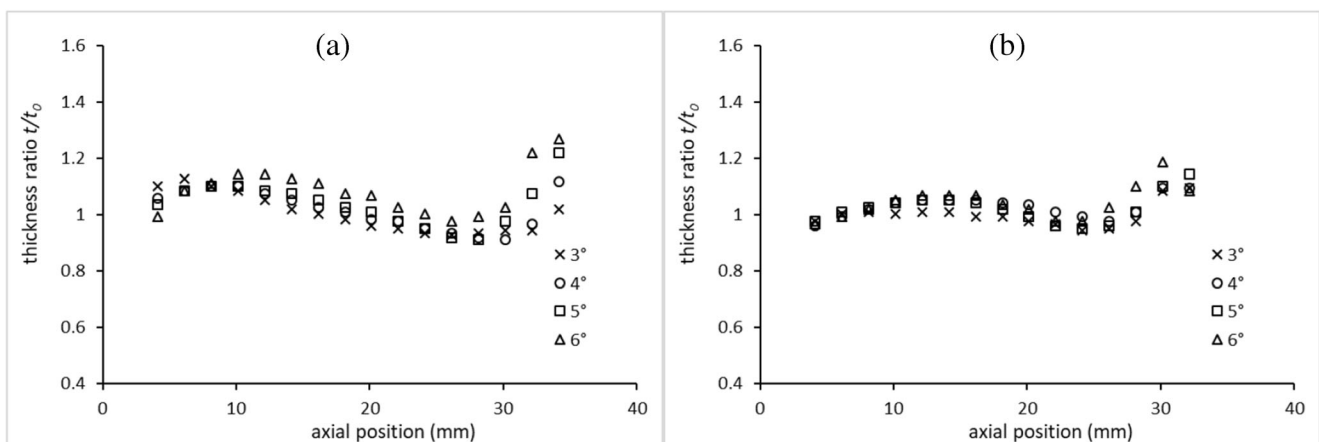


Fig. 21 Axial distributions of thickness ratio along two sides of the wall with different $\Delta\theta$ when $\varphi = 72^\circ$: **a** lower side and **b** upper side

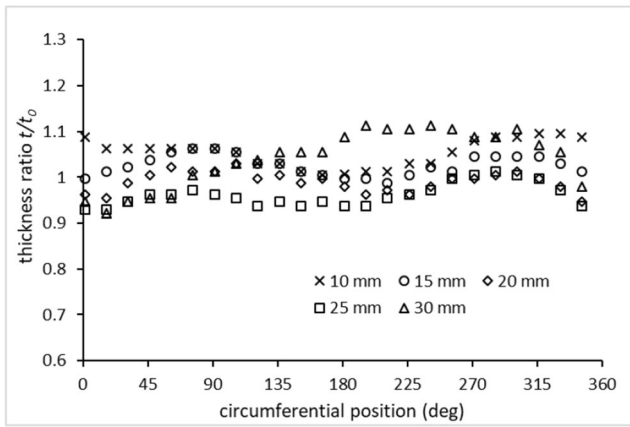


Fig. 22 Circumferential distributions of thickness ratio at different positions on the wall

4.2 Axial distribution of wall thickness

The experiments on cylindrical cups using the rotational pass set in asymmetric spinning were conducted with the parameters given in Table 2. For comparison, cylindrical cups using the same pass set in conventional spinning were formed.

An example of the formed product using the rotational pass set is shown in Fig. 18. The thickness on the upper and lower sides of the wall (t_U and t_L shown in Fig. 17) were measured axially. Figures 19 and 20 show the axial distribution of wall thickness ratios (t_U/t_0 and t_L/t_0) with different parameters of $\Delta\theta = 3^\circ, 4^\circ, 5^\circ, 6^\circ$ mm and $\varphi = 6^\circ, 24^\circ, 48^\circ, 72^\circ$. The dotted lines are distributions of thickness ratio (t_C/t_0) in conventional spinning (when $\varphi = 0^\circ$). The distributions of t_U/t_0 and t_L/t_0 are similar to t_C/t_0 . The difference between t_U/t_0 and t_L/t_0 is caused

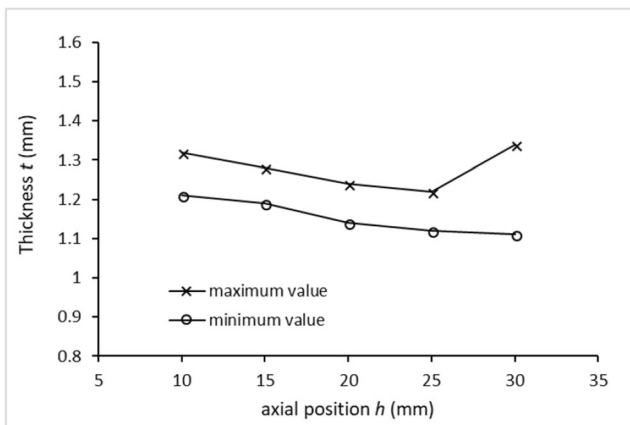


Fig. 23 Maximum and minimum values of circumferential thickness at different positions on the wall

by the varying half cone angle of the product during forming. The difference is much smaller compared with that in the translational pass set and it increased slightly as φ increased as shown in Fig. 19a–d. There is no obvious change in the difference between t_U/t_0 and t_L/t_0 as the incremental angle $\Delta\theta$ increased whereas the uniformity of the wall thickness decreased as shown in Fig. 20a–d. The thickness distributions on each side of the product with different $\Delta\theta$ when $\varphi = 72^\circ$ are compared in Fig. 21. The wall thickness increases as $\Delta\theta$ increases on both sides of the product.

4.3 Circumferential distribution of wall thickness

The circumferential distributions of thickness ratio (t/t_0) of the product formed with parameters of $\Delta\theta = 3^\circ, \varphi = 72^\circ$ at $h = 10, 15, 20, 25,$ and 30 mm are illustrated in Fig. 22. In rotational pass, the roller’s back-and-forth movement is weaker than that in translational pass set; therefore, the symmetry of the thickness distribution is better. The maximum and minimum values of circumferential thickness are illustrated in Fig. 23. The range of circumferential distribution of stays around 0.1 mm when $h = 10, 15, 20,$ and 25 mm and it increases to 0.23 mm when $h = 30$ mm due to the increase of the maximum value.

4.4 Product height

The circumferential distributions of product heights in terms of φ and $\Delta\theta$ are shown in Fig. 24 a and b respectively. The maximum and minimum values of product heights are shown in Fig. 25. The maximum values and minimum values show up around 0° directions and 180° directions respectively. The product heights distributions have a bathtub shape. Figure 24a indicates that the shape gets smoother when a smaller φ is used. A greater $\Delta\theta$ results in smaller heights and a smoother distribution as shown in Fig. 24b. The range of the distribution of product heights is small when $\varphi = 6^\circ$; however, they are nearly the same when $\varphi = 24^\circ, 48^\circ,$ and 72° as shown in Fig. 25a. The range gets smaller as $\Delta\theta$ increases as shown in Fig. 25b.

4.5 Forming limit

The forming experiments were investigated in terms of $\Delta\theta, f,$ and φ . Examples of wrinkle failures are shown in Fig. 26. The result of forming limit is illustrated in Fig. 27a–d. All the failures are wrinkles and no fracture was observed. A smaller f and $\Delta\theta$ should be used to avoid wrinkling. However, $\Delta\theta$ does not affect formability when $f = 1$ mm/rev. During the experiments, wrinkles tended to occur before φ reached its

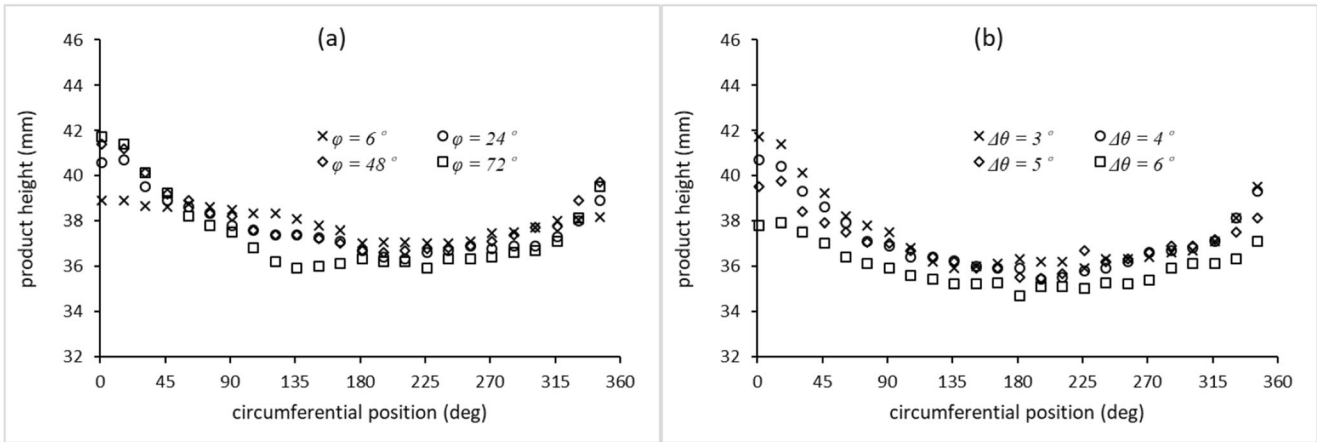


Fig. 24 Circumferential distributions of product heights: **a** with different φ when $\Delta\theta = 6^\circ$ and **b** with different $\Delta\theta$ when $\varphi = 72^\circ$

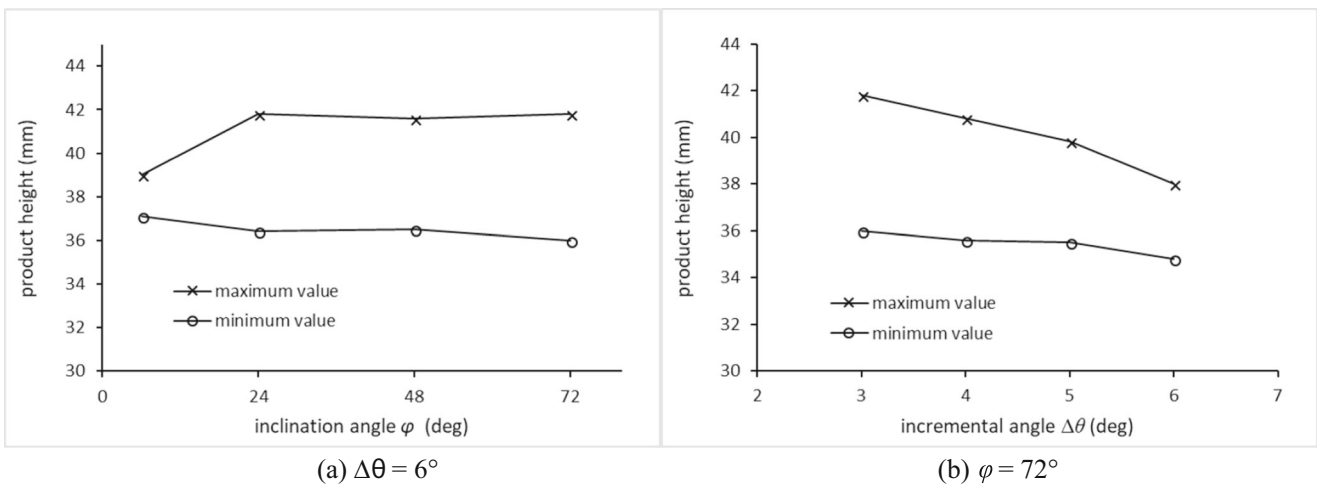


Fig. 25 Maximum and minimum values of circumferential product heights: **a** with different φ when $\Delta\theta = 6^\circ$ and **b** with different $\Delta\theta$ when $\varphi = 72^\circ$

value; as a result, a greater φ did not affect the forming limit in this study.

5 Conclusion

Asymmetric multi-pass spinning experiments using two kinds of pass sets were conducted. The thickness distributions are

examined and the forming limits are investigated in this study. The conclusions are as follows:

1. In the translational pass set, the difference between the axial distributions on two sides of the wall decreases as the pass pitch increases near the top of the product, and it increases near the edge of the wall. The difference increases as the inclination angle increases.

Fig. 26 Examples of failed products using the rotational pass set



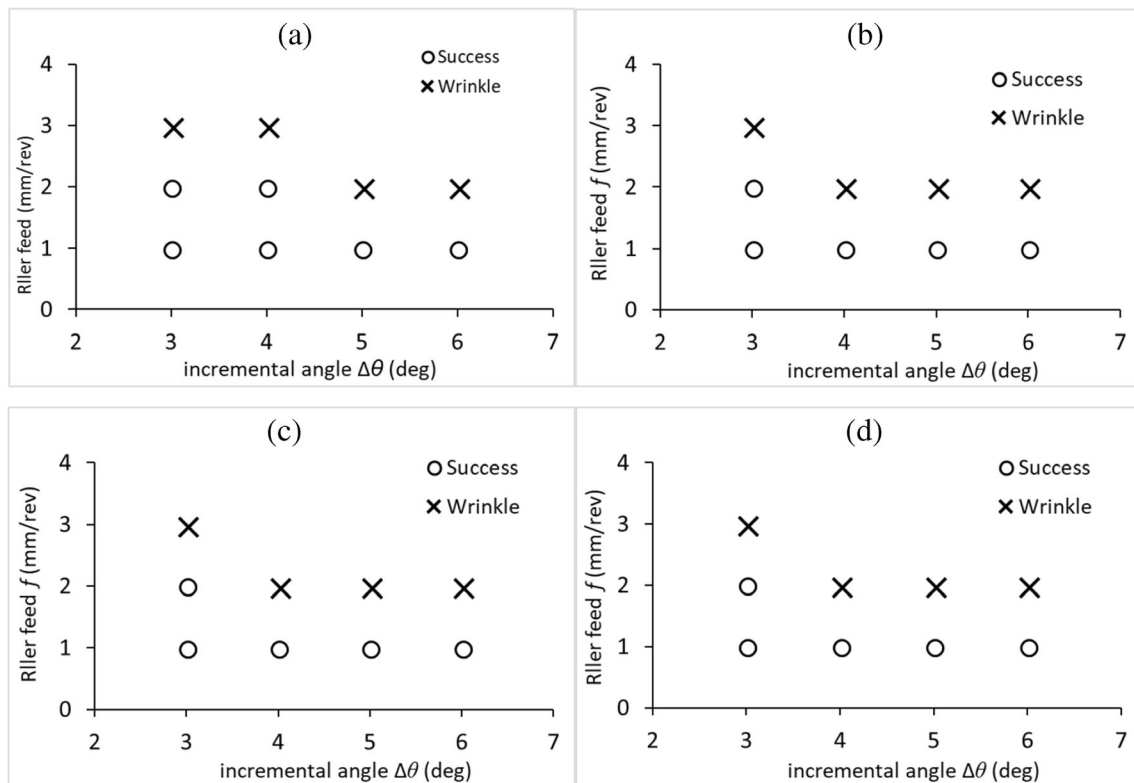


Fig. 27 Forming limit with different combinations of parameters: **a** $\varphi = 0^\circ$, **b** $\varphi = 24^\circ$, **c** $\varphi = 48^\circ$, and **d** $\varphi = 72^\circ$

- In the rotational pass set, the difference between the axial distributions on two sides of the wall is much smaller compared with that in the translational pass set. A greater inclination angle would cause a greater difference. A greater incremental angle does not affect the difference but reduces the uniformity of the wall thickness.
- The difference of the circumferential thickness of the wall increases towards the edge of the wall in both pass sets. The circumferential distributions of wall thickness are not symmetric.
- The unevenness of the height of the products formed in the translational pass set is much greater than that in a rotational pass set. The heights are smaller in the rotational pass set than that in a translational pass set.
- All the failures are wrinkles in the experiments. Wrinkles occur when the pass pitch or the roller feed ratio is too large. A greater inclination angle reduces the forming limit in the translational pass set and does not affect the forming limit in a rotational pass set.

Funding information This work was financially supported by the Chinese Aeronautical Establishment [2018ZE54028].

References

- Amano T, Tamura K (1984) The study of an elliptical cone spinning by the trial equipment. In: Proceedings of the 3rd international conference on rotary metalworking processes. Kyoto, Japan, pp. 213–224
- Gao XC, Kang DC, Meng XF, Wu HJ (1999) Experimental research on a new technology—ellipse spinning. *J Mater Process Technol* 94(2–3):197–200
- Xia Q, Lai Z, Zhan X, Cheng X (2010) Research on spinning method of hollow part with triangle arc-type cross section based on profiling driving. *Steel Res Int* 81(9):994–998
- Arai, H (2005) Robotic metal spinning—forming asymmetric products using force control. In: Proceedings of 2005 IEEE International Conference on Robotics and Automation. Barcelona, Spain. pp. 2702–2707
- Jia Z, Han ZR, Xu Q, Peng WF (2014) Numerical simulation and experiment study on hollow spinning process for square cross-section cone. *Int J Adv Manuf Technol* 75:1605–1612
- Sugita Y, Arai H (2015) Formability in synchronous multipass spinning using simple pass set. *J Mater Process Technol* 217, 336–344
- Sekiguchi A, Arai H (2012) Control of wall thickness distribution by oblique shear spinning methods. *J Mater Process Technol* 212(4):786–793
- Han ZR, Fan ZJ, Xiao Y, Jia Z (2016) A research on thickness distribution of oblique cone in dieless shear spinning. *Int J Adv Manuf Technol* 90:2901–2912
- Arai H, Kanazawa T (2018) Synchronous multipass spinning of oblique-bottom shape. *J Mater Process Technol* 260:66–76
- Xiao Y, Han ZR, Fan ZJ, Jia Z (2018) A study of asymmetric multipass spinning for angled-flange cylinder. *J Mater Process Technol* 256:202–215

Publisher's note Springer Nature remains neutral with regard to jurisdictional claims in published maps and institutional affiliations.